

Thermodynamics and structure of liquid metals: a critical assessment of the charged-hard-sphere reference system

This article has been downloaded from IOPscience. Please scroll down to see the full text article.

1992 J. Phys.: Condens. Matter 4 6173

(<http://iopscience.iop.org/0953-8984/4/29/003>)

View [the table of contents for this issue](#), or go to the [journal homepage](#) for more

Download details:

IP Address: 171.66.16.159

The article was downloaded on 12/05/2010 at 12:22

Please note that [terms and conditions apply](#).

Thermodynamics and structure of liquid metals: a critical assessment of the charged-hard-sphere reference system

Z Badirkhan†, O Akinlade†||, G Pastore‡ and M P Tosi§

† International Centre for Theoretical Physics, I-34014 Trieste, Italy

‡ Department of Theoretical Physics of the University of Trieste, I-34014 Trieste, Italy

§ Scuola Normale Superiore, I-56100 Pisa, Italy

Received 30 March 1992

Abstract. We calculate the Helmholtz free energies of the liquid alkali metals at various temperatures and those of several polyvalent metals (Mg, Cd, Al, In, Tl and Pb) near freezing, using the variational approach based on the Gibbs–Bogoliubov inequality in conjunction with the charged-hard-sphere reference fluid and with *ab initio* non-local pseudopotentials for the electron–ion interactions. The reference fluid introduces two variational parameters, i.e. the plasma coupling strength Γ and the packing fraction η , and is treated by a thermodynamically self-consistent approach which reduces to a highly accurate description of the one-component classical plasma for $\eta = 0$ and of the neutral-hard-sphere fluid for $\Gamma = 0$. For the alkali metals near freezing the free energy shows two competing minima as a function of these parameters, the first lying at $\eta \approx 0.42$ and $\Gamma \approx 120$ and the second near $\eta \approx 0.05$ and $\Gamma \approx 150$. The latter minimum provides the lowest variational bound to the free energy in all cases. A moderate increase in temperature shifts the absolute minimum of the free energy to $\eta = 0$ and removes the secondary minimum. Our results for the alkalis thus confirm the variational justification for a plasma-like viewpoint and also the good accuracy of such a description in comparison with experimental data on the liquid structure factor and on the excess entropy near freezing. For polyvalent metals the effective ion–ion potential in the region of the first-neighbour distance may show either a relatively deep attractive well or a soft-repulsion hump followed by a shallow minimum, depending on the electronic screening function used in its construction. However, the free-energy contours in the (η, Γ) plane are found to be quite insensitive to such differences in the pair potential shape. The relevant free-energy minima mostly lie near $\eta \approx 0.42$ and $\Gamma \approx 30$ and near $\eta = 0$ and $\Gamma \approx 160$. The free-energy differences between these minima, though very small, favour a plasma-like viewpoint for all the polyvalent metals that we have considered, except for Al. Both minima in the free energy lead to reasonable agreement with the available data on the excess entropy and the liquid structure factor. It thus appears that a plasma-like viewpoint and a hard-sphere viewpoint are similarly justifiable and useful for simple polyvalent metals.

1. Introduction

A widely used approach to determining the thermodynamic and structural properties of liquid metals is based on the Gibbs–Bogoliubov inequality, stating that the Helmholtz free energy is bounded from above by the sum of (i) the free energy of a reference system, and (ii) the difference in mean potential energy between the

|| Permanent address: Department of Physics, University of Agriculture, Abeokuta, Nigeria.

actual system and the reference system as evaluated on the distribution function of the latter [1]. Both the entropy and the structure factor of the liquid metal are, in this approach, those of the reference fluid at the variationally optimized values of its parameters. The main usefulness of the method lies in providing a relatively simple and direct variational estimate of the free energy of the liquid metal from a reasonably appropriate choice of the reference fluid. This thermodynamic function is not readily accessible by integral equations or computer simulation techniques, owing, in particular, to the dependence of the effective ion-ion potential on density.

The early work in this area adopted as a reference the fluid of neutral hard spheres (NHS), which is described by the packing fraction parameter $\eta = \pi\rho\sigma^3/6$, with ρ the atom number density and σ the hard sphere diameter [2–4]. Its free energy is available analytically as a fit to simulation data [5] and its structure factor as analytically given by the Percus–Yevick (PY) approximation is in qualitative accord with experiment for many liquid metals [6]. Subsequent work proposed the one-component classical plasma (OCP) of point charges on a uniform neutralizing background as an alternative reference fluid, especially suited for the alkali metals [7–10]. The OCP is described by the coupling strength parameter $\Gamma = Z^2e^2/(ak_B T)$, Z being the ionic valence and $a = (4\pi\rho/3)^{-1/3}$ the ion sphere radius, and its properties are known with high precision from computer simulation [11, 12]. Mon *et al* [13] comparatively discussed the merits of the NHS and OCP reference systems for liquid Na as a paradigm of the alkali metals and of liquid Al as a paradigm of polyvalent simple metals. Their calculations adopted the PY structure factor for the NHS and the hypernetted chain (HNC) approximation for the OCP. Using the empty-core pseudopotential and taking into account exchange and correlation in its screening by the conduction electrons, they concluded that the OCP gives a lower variational bound to the free energy and a better account of the liquid structure factor for Na, whereas Al is better described by the NHS reference system. This result has been taken to imply a real distinction between monovalent and polyvalent metals, which would be associated with the greater stiffness of the repulsive ionic cores in the latter.

Naturally enough, in the more recent literature, the one-component classical fluid of charged hard spheres (CHS) on a uniform neutralizing background has been extensively adopted as the reference system for liquid metals [14–23]. The CHS is described by the two parameters η and Γ and allows an effective interpolation between the NHS and the OCP, provided that its thermodynamic and structural properties are determined with sufficient accuracy. Work on liquid metals has generally made use of the analytic solution given for the CHS by Palmer and Weeks [24] in the mean spherical approximation (MSA), although some authors [19, 20, 22] have drawn attention to the limitations of the MSA solution with special regard to its lack of internal thermodynamic consistency in the values of the compressibility from the free energy, from the virial theorem, and from fluctuation theory. It has been reported [22] that starting from the NHS reference system and taking advantage of the two variational parameters inherent in the CHS leads to only limited improvement in the calculated thermodynamic functions for liquid alkali metals, unless some approximate account is taken of the requirement of thermodynamic consistency for the CHS. Moreover, the MSA is grossly wrong in the region of low η and large Γ , i.e. on the approach to the OCP reference system, since in this region it yields negative values for the radial distribution function near contact.

The aim of the present work is to examine in precise detail the merits of the CHS as a reference fluid interpolating between the NHS and the OCP, both for the alkalis

and for a number of polyvalent simple metals. To this end we use a very accurate description of the CHS, following recent work by some of us [25] which has developed alternative ways of enforcing thermodynamic consistency in the statistical mechanical theory of this model fluid and has shown that the results account for computer simulation data by Hansen and Weis [26] on the internal energy and the radial distribution function. Specifically, we adopt a modified hypernetted chain (MHNC) approximation, as originally proposed by Rosenfeld and Ashcroft [27], in which we construct the bridge function for the CHS from the results of Verlet and Weis [28] and Henderson and Grundke [29] for the NHS. Thus, in the limit $\Gamma = 0$ our treatment of the CHS reduces to a very accurate description of the thermodynamic and structural properties of the NHS, yielding in particular the Carnahan–Starling equation of state. We also find that in the limit $\eta = 0$ our results are in very close agreement with the most accurate computer simulation data presently available for the OCP [12]. The possibility of describing the OCP by an MHNC treatment involving an NHS-like bridge function was first demonstrated by Rosenfeld and Ashcroft [27], using PY results for the NHS correlation functions.

The effective ion–ion interactions in the liquid metal are also treated in the present work at a comparable level of sophistication. We use the modified generalized non-local model pseudopotential (GNMP) of Li *et al* [30], the reliability of which has already been demonstrated in a number of other recent calculations of metallic properties. For metals in which the electron–ion interactions are especially strong, i.e. in Li and polyvalent metals, Li *et al* [30, 31] have made various efforts to incorporate higher-order perturbation effects in the GNMP, so our results transcend to some extent the usual low-order perturbation theory. As for the electronic screening functions, we have adopted the well established form of the exchange and correlation factor due to Singwi *et al* for the alkalis [32]. For polyvalent metals, on the other hand, different screening functions may yield qualitatively different shapes for the effective ion–ion potential in the region of the first-neighbour distance. We have accordingly adopted two alternative forms for the exchange and correlation factors for these metals, considering in addition to that of Singwi *et al* the form due to Ichimaru and Utsumi [33].

The layout of the paper is briefly as follows. In section 2 we summarize the essential aspects of the theory and give some details of our treatment of the CHS reference system, leading to a tabulation of its excess energy and entropy as functions of η and Γ . In section 3 we report and discuss our numerical results for the alkali metals near freezing and at a few somewhat higher temperatures, while in section 4 we present our results for the polyvalent metals Mg, Cd, Al, In, Tl and Pb near freezing. Finally, in section 5 we summarize our main conclusions.

2. Theory

In this section we summarily present the main expressions and CHS results that will be needed in our calculations for liquid metals. Adopting the CHS reference system and the GNMP, the free energy of the liquid metal as a function of η and Γ is written as

$$F(\eta, \Gamma) = E_{\text{EG}} + F_{\text{d}} - \frac{1}{\pi} Z_{\text{eff}}^2 \times \int_0^\infty dq S_{\text{CHS}}(q) G_{\text{EC}}(q) + F_{\text{NHS}} + F_{\text{CHS}}^{\text{ex}} + \frac{Z_{\text{eff}}^2 - Z^2}{Z^2} U_{\text{CHS}}^{\text{ex}}. \quad (1)$$

Here, E_{EG} is the ground state energy of the degenerate electron gas, F_d is the non-local contribution arising from the deviation of the electron-ion pseudopotential from a purely Coulombic form, $G_{EG}(q)$ is the normalized energy-wavenumber characteristic, and $Z_{eff} = (Z^2 - \rho_d^2)^{1/2}$, Z and ρ_d being the nominal ionic valence and the depletion charge density. The explicit form of these quantities can be found in [4] and is therefore not given here. The other quantities in (1) are the structure factor $S_{CHS}(q)$ of the CHS, its excess free energy F_{CHS}^{ex} and excess internal energy U_{CHS}^{ex} , and the free energy F_{NHS} of the NHS, which in the Carnahan–Starling equation of state is given by

$$F_{NHS} = F_{id} + k_B T \eta(4 - 3\eta)/(1 - \eta)^2 \quad (2)$$

F_{id} being the free energy of the ideal classical gas. The expression (1) is minimized with respect to η and Γ , in order to obtain a variational upper bound to the free energy of the liquid metal at a given temperature and density.

The structure of the CHS at a given η and Γ is evaluated in the MHNC [25]. We use the exact equations

$$h(r) = c(r) + \rho \int d\mathbf{r}' c(|\mathbf{r} - \mathbf{r}'|) h(\mathbf{r}') \quad (3)$$

and

$$y(r) = \exp[-\beta\phi_c(r) + h(r) - c(r) - b(r)] \quad (4)$$

where $g(r)$ and $h(r) = g(r) - 1$ are the radial distribution function and the pair correlation function, $c(r)$ is the Ornstein–Zernike direct correlation function, $y(r) = g(r) \exp[\beta\phi_r(r)]$ with $\phi_r(r)$ the hard sphere potential and $\beta = (k_B T)^{-1}$, $\beta\phi_c(r) = \Gamma a/r$ and $b(r)$ is the bridge function. The latter is approximately evaluated from the expressions

$$\begin{aligned} b(r) &= -1 - c_{VW}(r) - \ln \{g_{VW}(r) \exp[\beta\phi_r(r)]\} & (r < \sigma) \\ &= h_{VW}(r) - c_{VW}(r) - \ln g_{VW}(r) & (r > \sigma). \end{aligned} \quad (5)$$

Here, $g_{VW}(r)$ and $c_{VW}(r)$ are the Verlet–Weis results for the radial distribution function and the direct correlation function of the NHS at a packing fraction η^* , which is determined by the requirement of consistency for the compressibility from the virial theorem and from fluctuation theory. In solving the combined equations (3)–(5) in conjunction with the requirement of thermodynamic consistency, we have used the numerical algorithm developed by Gillan and Abernethy [34, 35], with 2049 mesh points and a grid size $\Delta r = 0.025a$. We have also taken account of the density dependence of the bridge function. Our results are therefore slightly more accurate than those obtained earlier [25] in the same approach.

The excess internal energy per particle of the CHS is given by

$$\beta U_{CHS}^{ex} = \frac{1}{2} \rho \Gamma \int d\mathbf{r} \frac{a}{r} [g_{CHS}(r) - 1] \quad (6)$$

and its excess free energy follows from this by integration over the coupling strength Γ . In carrying out the integration over Γ we have followed the method first suggested

Table 1. Excess internal energy $-\beta U_{\text{CHS}}^{\text{ex}}$ of the fluid of charged hard spheres as a function of the parameters Γ and η .

$\Gamma \backslash \eta$	0	0.2	0.343	0.4	0.425	0.45	0.475	0.50
0	0	0	0	0	0	0	0	0
2	1.3228	1.5571	1.6741	1.7070	1.7190	1.7268	1.7375	1.7436
4	2.9333	3.1848	3.3687	3.4255	3.4474	3.4610	3.4802	3.4913
6	4.5982	4.8415	5.0741	5.1502	5.1807	5.1995	5.2258	5.2414
10	8.0060	8.2086	8.5056	8.6128	8.6562	8.6860	8.7243	8.7466
15	12.323	12.480	12.817	12.957	13.016	13.054	13.109	13.136
20	16.672	16.795	17.155	17.316	17.384	17.436	17.499	17.533
30	25.441	25.504	25.860	26.058	26.152	26.221	26.304	26.350
40	34.254	34.283	34.613	34.830	34.936	35.028	35.127	35.182
50	43.093	43.103	43.387	43.625	43.735	43.843	43.959	44.028
60	51.935	51.945	52.195	52.428	52.561	52.683	52.802	52.885
70	60.808	60.813	61.011	61.244	61.395	61.532	61.655	61.747
80	69.692	69.694	69.861	70.085	70.230	70.404	70.514	70.613
90	78.572	78.580	78.716	78.932	79.078	79.274	79.403	79.489
100	87.484	87.486	87.575	87.778	87.935	88.140	88.285	88.379
120	105.29	105.29	105.36	105.50	105.71	105.89	106.08	106.19
160	140.99	140.99	140.99	141.05	141.27	141.51	141.67	141.89
200	176.69	176.69	176.69	176.71	176.90	177.13	177.43	177.55
220	194.59	194.59	194.56	194.50	194.72	194.99	195.31	195.40
250	221.40	221.40	221.35	221.34	221.60	221.82	222.07	222.26

by Hansen [36] for the OCP, which involves using a very fine integration mesh in the range $0 < \Gamma \leq 1$ and a coarser mesh at larger Γ . Our numerical results for the excess internal energy and excess entropy of the CHS are reported in tables 1 and 2, respectively. Interpolation between the values given in the tables can be effected rather accurately by a three-point divided difference method, as confirmed by comparison with the recent simulation data of Penfold *et al* [37] at $\eta = 0.4$ and low Γ .

There is excellent agreement between our results shown in table 1 and the simulation data on the excess energy of the CHS as reported by Hansen and Weis [26] at a few values of η and Γ in the range of parameters of interest here. Of course, the comparison with simulation data cannot be a test of our results to the number of significant digits that we have given. As we shall see, the free energy needs to be calculated to at least four significant digits for a comparative variational assessment of different reference systems.

The properties of the OCP limit at $\eta = 0$, as known from computer simulation, have not been built in any way into our description of the CHS. Comparison of our results with the OCP data of DeWitt *et al* [12] shows agreement for the excess internal energy to four significant digits and for the excess entropy to the second decimal figure. The values of the OCP free energy from simulation are in fact slightly lower than those obtained from the present treatment.

3. Results for the alkali metals

3.1. Thermodynamic and structural properties near freezing

Figure 1 shows the contours of the free energy in the (η, Γ) plane for liquid Na near freezing (at $T = 373$ K). The separation between neighbouring contour lines

Table 2. Excess entropy $-S_{\text{CHS}}^{\text{ex}}/k_{\text{B}}$ of the fluid of charged hard spheres as a function of the parameters Γ and η .

$\Gamma \backslash \eta$	0	0.2	0.343	0.4	0.425	0.45	0.475	0.50
0	0	1.062	2.361	3.111	3.503	3.942	4.438	5.000
2	0.264	1.086	2.367	3.115	3.506	3.944	4.439	5.001
4	0.474	1.138	2.382	3.123	3.513	3.950	4.443	5.004
6	0.636	1.191	2.400	3.133	3.521	3.956	4.448	5.008
10	0.902	1.300	2.438	3.156	3.538	3.972	4.459	5.017
15	1.158	1.437	2.487	3.187	3.564	3.993	4.478	5.030
20	1.367	1.572	2.543	3.222	3.590	4.020	4.495	5.046
30	1.720	1.828	2.648	3.292	3.652	4.075	4.542	5.088
40	2.008	2.069	2.764	3.366	3.709	4.132	4.589	5.130
50	2.255	2.291	2.873	3.445	3.768	4.185	4.635	5.176
60	2.459	2.494	2.992	3.516	3.841	4.251	4.681	5.223
70	2.660	2.689	3.101	3.588	3.909	4.313	4.730	5.267
80	2.844	2.870	3.226	3.674	3.969	4.390	4.778	5.309
90	3.002	3.034	3.341	3.755	4.035	4.456	4.848	5.355
100	3.175	3.200	3.448	3.828	4.102	4.511	4.905	5.411
120	3.457	3.479	3.691	3.981	4.275	4.621	5.027	5.534
160	3.977	3.999	4.141	4.311	4.551	4.903	5.229	5.798
200	4.390	4.413	4.544	4.665	4.832	5.122	5.540	5.966
220	4.606	4.627	4.735	4.780	4.957	5.266	5.674	6.055
250	4.862	4.885	4.978	5.085	5.266	5.487	5.787	6.257

corresponds to $\Delta F = 1 \times 10^{-4}$ au. The free energy has two very broad minima, the first located at $\eta = 0.047$ and $\Gamma = 151$ and the second at $\eta = 0.424$ and $\Gamma = 123$. The free energy at the first minimum is deeper by 3×10^{-4} au and is almost indistinguishable from the free energy that we obtain with the OCP reference system, i.e. by searching for a minimum along the $\eta = 0$ axis. The secondary CHS minimum, on the other hand, is well separated both in its location and in its free energy value from the NHS results, which are obtained by searching for a minimum along the $\Gamma = 0$ axis. We also remark that (i) our free energy value at the secondary CHS minimum is lower than that obtained in earlier calculations based on the MSA [22], and (ii) the absolute CHS minimum lies in the region of η where the MSA is completely unreliable and therefore its presence is a consequence of our accurate treatment of the CHS reference system.

The above results for Na are typical of those obtained for all the alkali metals near freezing, as reported in table 3. In all cases we find that the absolute minimum of the free energy lies very close to the OCP. The variationally optimized values of Γ , though appreciably higher than those obtained in previous calculations, are still significantly lower than the value $e^2/(ak_{\text{B}}T)$ that one would calculate from the nominal ionic valence and the thermodynamic state of the metal. This quantity ranges from 181 for Cs to 209 for Li.

In table 3 we also compare our results for the free energy F , the internal energy U and the excess entropy s of each liquid alkali with experimental data [22, 23]. There is complete agreement with experiment for the free energies of Na, K and Rb, while for Li and Cs the discrepancy between theory and experiment is at the level of 1×10^{-3} au. We notice that the differences in the theoretical results obtained for F with different reference systems are of this same magnitude. In partitioning the calculated free energy into its internal energy and entropy contributions, however,

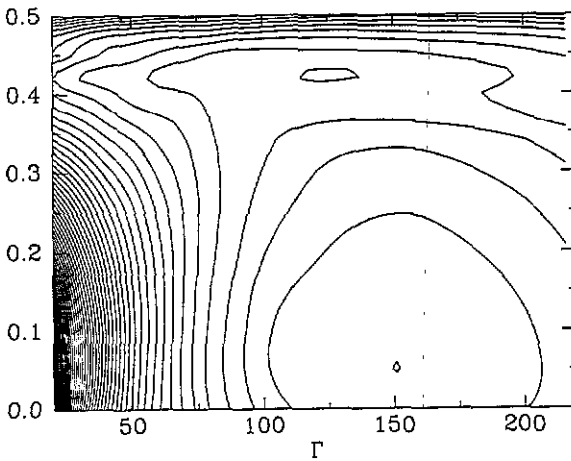


Figure 1. Free-energy contours for liquid Na at $T = 373$ K in the (η, Γ) plane for $\Gamma \geq 20$. The separation between neighbouring contour lines corresponds to $\Delta F = 1 \times 10^{-4}$ au.

Table 3. Location of free energy minima in the (η, Γ) plane for the alkali metals near freezing, and corresponding values of the Helmholtz free energy F , the internal energy U and the excess entropy s , compared with experimental values. Assumed values of η or Γ , corresponding to a one-dimensional minimization along the appropriate coordinate axis, are marked with asterisks.

	η	Γ	$-F(\text{au})$	$-F_{\text{exp}}(\text{au})$	$-U(\text{au})$	$-U_{\text{exp}}(\text{au})$	$-s/k_B$	$-s_{\text{exp}}/k_B$
Li	0*	160	0.2660	0.265	0.2584	0.254	3.98	3.7, 3.54
	0.052	160	0.2660		0.2584		3.99	
	0.425	138	0.2656		0.2586		4.41	
	0.467	0*	0.2647		0.2575		4.27	
Na	0*	153	0.2357	0.236	0.2271	0.232	3.89	3.45
	0.047	151	0.2358		0.2271		3.88	
	0.424	123	0.2355		0.2273		4.29	
	0.438	0*	0.2349		0.2261		3.72	
K	0*	145	0.2011	0.201	0.1918	0.1956	3.80	3.45
	0.054	144	0.2011		0.1918		3.80	
	0.423	121	0.2008		0.1921		4.25	
	0.438	0*	0.2004		0.1910		3.72	
Rb	0*	138	0.1929	0.193	0.1829	0.1870	3.71	3.63
	0.051	135	0.1929		0.1829		3.68	
	0.418	120	0.1926		0.1831		4.18	
	0.435	0*	0.1922		0.1822		3.67	
Cs	0*	145	0.1810	0.182	0.1707	0.1757	3.79	3.56
	0.050	143	0.1811		0.1707		3.79	
	0.416	120	0.1808		0.1708		4.16	
	0.441	0*	0.1803		0.1700		3.78	

the results are not of a similarly high accuracy when compared with the data. In particular, there is a clear tendency in the theory to overestimate the magnitude of

Table 4. Locations of maxima and minima (\AA^{-1}) in the liquid structure factor of the alkali metals near freezing. Experimental data (from van der Lugt and Ablas [38]) are given in the first row, while the results obtained with the CHS (or the OCP) and the NHS reference system are given in the second and third row, respectively. The locations of maxima are in the first three columns and those of minima in the last two columns.

	1st	2nd	3rd	1st	2nd
Li	2.50	4.65	6.90	3.50	5.75
	2.45	4.50	6.60	3.40	5.70
	2.50	4.75	7.05	3.55	5.90
Na	2.05	3.75	5.60	2.75	4.65
	2.00	3.70	5.45	2.80	4.65
	2.10	3.95	5.90	2.95	4.90
K	1.65	2.95	4.45	2.25	3.75
	1.60	3.00	4.40	2.25	3.75
	1.70	3.20	4.75	2.40	3.95
Rb	1.50	2.80	4.20	2.10	3.50
	1.50	2.80	4.10	2.10	3.50
	1.55	2.95	4.40	2.20	3.70
Cs	1.40	2.60	3.85	1.90	3.25
	1.40	2.60	3.80	1.95	3.25
	1.45	2.75	4.10	2.05	3.40

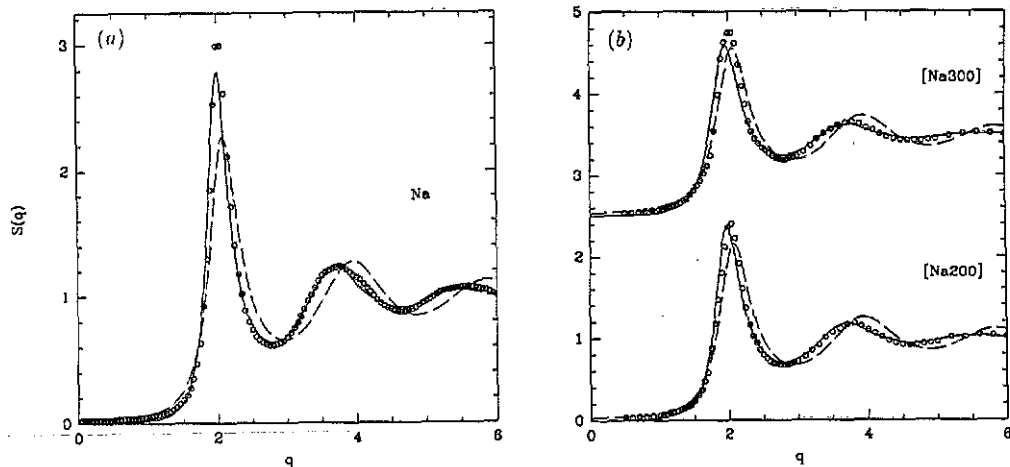


Figure 2. Liquid structure factor of Na from the CHS and OCP reference systems (full lines) and from the NHS reference system (dashes), in comparison with experiment (circles). (a): $T = 100\text{ }^{\circ}\text{C}$; (b): $T = 200\text{ }^{\circ}\text{C}$ and $300\text{ }^{\circ}\text{C}$.

the excess entropy, irrespective of the reference system.

The calculated structure factor of liquid Na near freezing, at the values of η and Γ corresponding to the absolute minimum of the free energy, is shown in figure 2(a) in comparison with the experimental data given by van der Lugt and Ablas [38]. There is a very marked improvement in the theoretical results in going from the NHS

to the CHS reference system, and the latter is practically indistinguishable from the OCP reference system. Again, these results for Na are fully illustrative of the case for all the liquid alkalis. In table 4 we report the locations of the structure factor maxima and minima near freezing for all the alkalis as have been obtained by us with the CHS and NHS reference systems, in comparison with the experimental data [38].

3.2. Thermodynamic and structural properties at higher temperatures

Figure 3 shows the contours of the free energy for liquid Na at $T = 573$ K. For this case there is a continuous drop in the free energy on going from the NHS to the OCP, i.e. the secondary CHS minimum has disappeared, and the only minimum lies at $\eta = 0$, $\Gamma = 82$. At intermediate temperature the absolute minimum of the free energy is still found to lie close to, but slightly removed from, the OCP. In table 5 the behaviour found for the thermodynamic functions of the liquid alkalis from Na to Cs with increasing temperature is illustrated.

Table 5. Location of free-energy minima in the (η, Γ) plane for alkali metals at temperatures above freezing and atomic volume Ω_0 (from data reported by Waseda [39]), and corresponding values of the free energy F , the internal energy U and the excess entropy s . Assumed values of η or Γ , corresponding to a one-dimensional minimization along the appropriate coordinate axis, are marked with asterisks.

	T (K)	Ω_0	η	Γ	$-F$ (au)	$-U$ (au)	$-s/k_B$
Na	473	285.264	0*	109	0.2382	0.2258	3.32
			0.062	105	0.2382	0.2258	3.31
			0.425	0*	0.2375	0.2253	3.50
	573	292.388	0	82	0.2409	0.2245	2.89
			0.411	0*	0.2401	0.2244	3.28
K	378	534.921	0*	123	0.2023	0.1912	3.50
			0.056	116	0.2023	0.1912	3.45
			0.428	0*	0.2015	0.1906	3.56
	473	549.686	0	92	0.2050	0.1900	3.04
			0.417	0*	0.2043	0.1898	3.37
Rb	373	661.366	0*	109	0.1948	0.1821	3.32
			0.062	106	0.1948	0.1822	3.33
			0.425	0*	0.1942	0.1817	3.50
	473	685.510	0	80	0.1982	0.1808	2.85
			0.408	0*	0.1975	0.1807	3.23
Cs	373	829.178	0*	109	0.1835	0.1697	3.31
			0.061	111	0.1835	0.1699	3.40
			0.425	0*	0.1828	0.1693	3.50
	473	856.356	0	80	0.1872	0.1685	2.86
			0.409	0*	0.1864	0.1683	3.24

As illustrated for Na in figure 2(b), our CHS results for the structure factor continue to be in very good agreement with the experimental data [39] over the limited temperature range that we have explored. Again the shape of the structure factor is appreciably distorted when one adopts the NHS reference system.

In summary, our results for the liquid alkalis at and above freezing fully confirm the appropriateness of the OCP reference system and the viewpoint that these liquid

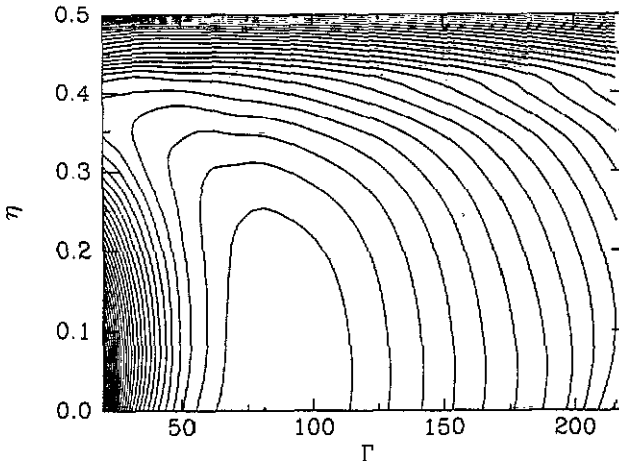


Figure 3. Free-energy contours for liquid Na at $T = 573$ K in the (η, Γ) plane for $\Gamma \geq 20$. The separation between neighbouring contour lines corresponds to $\Delta F = 1 \times 10^{-4}$ au.

metals are usefully looked upon as classical ionic plasmas screened by conduction electrons.

4. Results for polyvalent metals

As was reiterated in section 1, the effective ion-ion potential in polyvalent metals is very sensitive to the details of the exchange and correlation factor in the electronic screening function. In figure 4 this sensitivity for Mg and Al in comparison with Na is illustrated. In particular, in the case of Al, the replacement of the SSTL screening function [32] by the Ichimaru-Utsumi (IU) screening function [33] replaces a fairly deep attractive well in the region of the first-neighbour distance by a soft-repulsion hump. However, while different pair potentials lead to somewhat different values for the free energy, they do not affect the main features of the results in the search for free-energy minima in the (η, Γ) plane. Indeed, the structure-dependent contribution from the ion-ion interactions is a relatively small part of the total free energy. We shall therefore focus first on the results obtained with the SSTL-screened pair potentials.

Figure 5 shows the free energy contours in the (η, Γ) plane for liquid Mg near freezing, the separation between neighbouring contour lines being $\Delta F = 2 \times 10^{-4}$ au. We find three minima, the deepest one lying at $\eta = 0$, $\Gamma \approx 160$. The best reference system for this liquid metal, therefore, is still the OCP. A secondary CHS minimum lies at $\eta = 0.425$ and $\Gamma = 30$, i.e. fairly close to the NHS, which has its own minimum at $\eta = 0.432$. Another secondary minimum is found at $\eta = 0.45$ and $\Gamma = 90$. We discard the latter relative minimum from further consideration, on the grounds that such a combination of high η and high Γ (i) is leading us into a region of parameters where our CHS results may be not as accurate as elsewhere, and (ii) yields a severe overestimate for the degree of short-range order in the liquid metal, as can be seen from both the magnitude of the excess entropy and the peak heights in the structure factor.

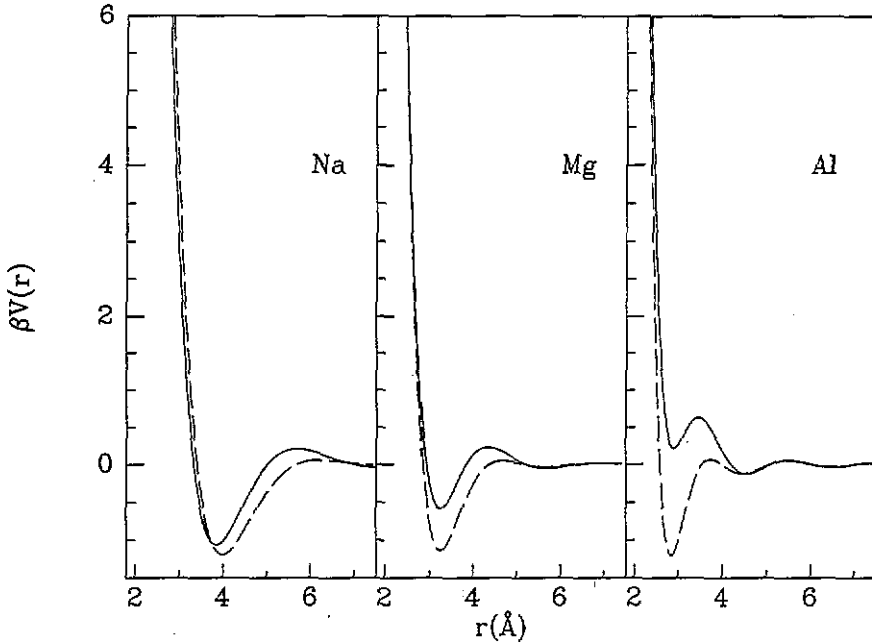


Figure 4. Pair potential $V(r)$, in units of $k_B T$ versus interatomic distance r in Na, Mg and Al, as calculated from SSTL screening (dashes) and from IU screening (full lines).

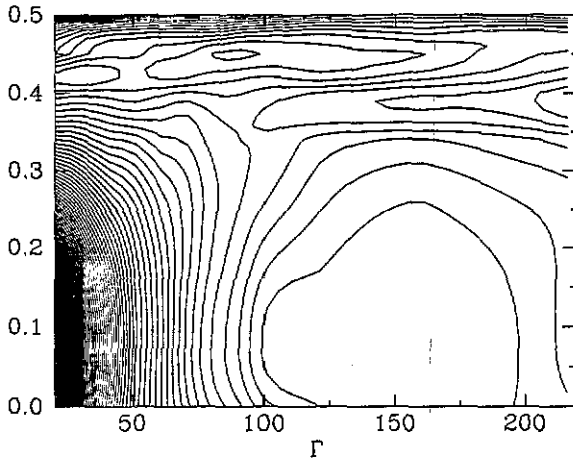


Figure 5. Free-energy contours for liquid Mg near freezing in the (η, Γ) plane for $\Gamma \geq 20$. The separation between neighbouring contour lines corresponds to $\Delta F = 2 \times 10^{-4}$ au.

For Al, the 'spurious' minimum (at $\eta = 0.478$ and $\Gamma = 218$) is slightly lower than the others. Discarding it for the reasons just given, we find acceptable minima at (i) $\eta = 0.431$ and $\Gamma = 0$, i.e. at the NHS; (ii) $\eta = 0$ and $\Gamma = 170$, i.e. at the OCP; and (iii) $\eta = 0.425$ and $\Gamma = 30$. The differences in free energy between these minima are at the level of 1×10^{-4} au, i.e. within the likely inaccuracy of our numerical results.

Table 6. Location of free-energy minima in the (η, Γ) plane for polyvalent metals near freezing, determined with SSTL screening, and corresponding values of the Helmholtz free energy F , the internal energy U and the excess entropy s , compared with experimental values. Assumed values of Γ , corresponding to a one-dimensional minimization along the η axis, are marked with asterisks.

	η	Γ	$-F$ (au)	$-F_{\text{exp}}$ (au)	$-U$ (au)	$-U_{\text{exp}}$ (au)	$-s/k_B$	$-s_{\text{exp}}/k_B$
Mg	0	160	0.8969	0.905	0.8719	0.879	3.98	3.45, 3.7
	0.425	30	0.8964		0.8704		3.65	
	0.432	0*	0.8961		0.8700		3.63	
Cd	0	160	0.9697	1.020	0.9502	1.000	3.97	4.15, 3.68
	0.425	30	0.9694		0.9494		3.65	
	0.426	0*	0.9693		0.9490		3.51	
Al	0	170	2.0759	2.060	2.0521	2.035	4.09	3.6, 3.61
	0.425	30	2.0758		2.0506		3.65	
	0.431	0	2.0760		2.0507		3.60	
In	0	212	2.0000	2.042	1.9878	2.030	4.52	4.4, 4.61
	0.425	30	1.9986		1.9852		3.65	
	0.432	0*	1.9983		1.9848		3.62	
Tl	0	160	2.0868	2.165	2.0666	2.145	3.98	4.05, 4.13
	0.425	30	2.0852		2.0643		3.65	
	0.425	0*	2.0849		2.0636		3.50	
Pb	0	160	3.5916	3.656	3.5702	3.634	3.98	4.1, 3.69
	0.425	30	3.5888		3.5667		3.65	
	0.425	0*	3.5885		3.5660		3.50	

The full set of results that we have obtained for six polyvalent simple metals is reported in table 6 (SSTL screening and E_{EG}) and table 7 (IU screening and E_{EG}). The following observations may be made.

(i) There is almost uniform regularity in the locations of the free energy minima, in contrast to the scatter of locations found in earlier calculations based on the MSA [23]. Our treatment of the CHS always yields a minimum at the OCP, lying in most cases near $\Gamma = 160$, as well as a minimum having η close to the optimized η of the NHS and Γ close to 30. However, the differences in free energy between these minima, as well as the differences between these free energies and the optimized NHS free energy, are extremely small.

(ii) If one takes as literally valid all the significant digits that we have reported for the free energy values, the OCP minimum is the lowest in all cases except for Al. Indeed, the acceptable absolute minimum of the free energy for this metal lies at the NHS. We notice that our results for Al have a second and more dubious distinguishing feature: the calculated upper bound for the free energy lies *below* the measured free energy.

(iii) Though the discrepancies between calculated and measured free energy are significantly larger than in the case of the alkalis, the agreement may still be considered as reasonable. The OCP reference system generally yields a fairly high value for the excess entropy, but the scatter in the experimental data appears to be too large for a safe assessment of the quality of this result.

Table 7. Location of free-energy minima in the (η, Γ) plane for polyvalent metals near freezing, determined with 1D screening, and corresponding values of the Helmholtz free energy F , the internal energy U and the excess entropy s , compared with experimental values. Assumed values of Γ , corresponding to a one-dimensional minimization along the η axis, are marked with asterisks.

	η	Γ	$-F$ (au)	$-F_{\text{exp}}$ (au)	$-U$ (au)	$-U_{\text{exp}}$ (au)	$-s/k_B$	$-s_{\text{exp}}/k_B$
Mg	0	160	0.8816	0.905	0.8565	0.879	3.98	3.45, 3.7
	0.425	30	0.8815		0.8555		3.65	
	0.428	0*	0.8813		0.8550		3.56	
Cd	0	110	0.9559	1.020	0.9352	1.000	3.32	4.15, 3.68
	0.422	30	0.9558		0.9357		3.61	
	0.425	0*	0.9558		0.9355		3.50	
Al	0	160	2.0632	2.060	2.0396	2.035	3.98	3.6, 3.61
	0.425	30	2.0634		2.0383		3.65	
	0.428	0	2.0636		2.0382		3.56	
In	0	160	1.9887	2.042	1.9758	2.030	3.98	4.4, 4.61
	0.425	30	1.9879		1.9741		3.65	
	0.429	0*	1.9871		1.9736		3.57	
Tl	0	160	2.0815	2.165	2.0612	2.145	3.98	4.05, 4.13
	0.424	30	2.0793		2.0587		3.64	
	0.425	0*	2.0789		2.0577		3.50	
Pb	0	160	3.6245	3.656	3.6030	3.634	3.98	4.1, 3.69
	0.425	30	3.6211		3.5991		3.65	
	0.425	0*	3.6205		3.5981		3.50	

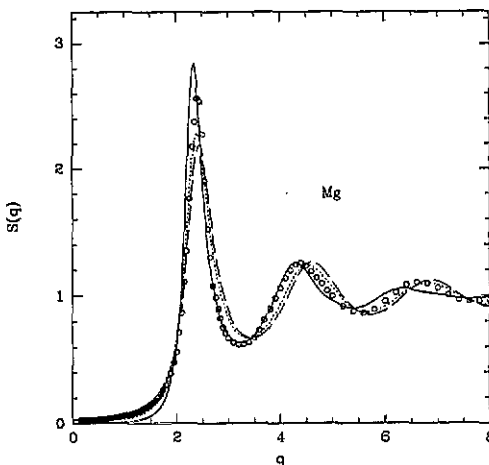


Figure 6. Liquid structure factor of Mg near freezing from the OCP reference system (full line), the CHS reference system (dotted line) and the NHS reference system (dashes), in comparison with experiment (circles).

Also from the structural point of view, it is hard to make a general statement about the relative merits of an OCP-like or an NHS-like viewpoint for polyvalent metals. Figures 6 and 7 show the calculated structure factors for liquid Mg and Al, respectively, in comparison with experimental data [39]. The OCP results appear to be

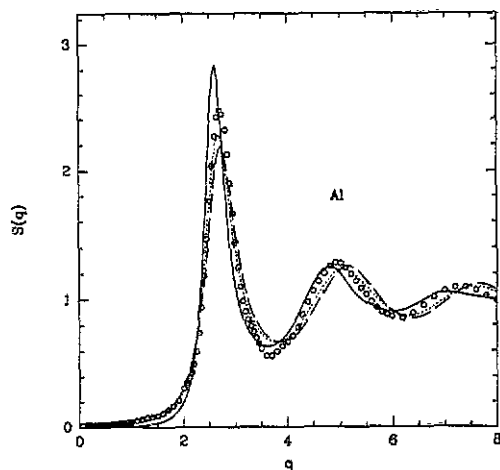


Figure 7. Liquid structure factor of Al near freezing from the OCP reference system (full line), the CHS reference system (dotted line) and the NHS reference system (dashes), in comparison with experiment (circles).

more satisfactory for the former metal and the NHS ones for the latter. Calculations of the liquid structure factor for Cd, In, Tl and Pb, that we have carried out but do not illustrate with additional figures, show essential competitiveness between the two reference systems, with perhaps a slight advantage for the NHS. The relationship between these structural results and the hardness of the repulsive core in each metal is not immediately obvious. In fact, while the core in Al is the hardest among the metals that we have considered, Mg is the second hardest.

5. Summary and concluding remarks

We have presented a very painstaking analysis of the CHS reference system in the context of variational calculations of the free energy for the liquid alkali metals and for several polyvalent simple metals. The analysis has been based on an accurate statistical mechanical treatment of the thermodynamic and structural properties of the CHS as a model fluid allowing interpolation between the NHS and the OCP. In this treatment we have incorporated the best available knowledge on the properties of the NHS fluid and have taken advantage of the fact that the OCP at strong coupling may be described accurately through NHS-like bridge functions. Our results for liquid metals therefore represent a major improvement in accuracy relative to earlier variational calculations using the PY approximation for the NHS, the HNC approximation for the OCP or the mean spherical approximation for the CHS.

Our results for the alkalis confirm that the OCP is a very satisfactory reference system. Only marginal improvement is found on replacing it by the CHS for these metals, and indeed the OCP becomes the variationally preferable reference system with increasing temperature.

For polyvalent metals, on the other hand, the OCP and an NHS-like CHS (or, more simply, the NHS) are essentially competitive. From a very strict variational viewpoint, only for Al could we justify the NHS as a reference system, while the OCP appears to be preferable for Mg, Cd, In, Tl and Pb. The two reference systems lead to somewhat different results for the excess entropy and the liquid structure factor, with the OCP predicting a somewhat higher degree of short-range order. Both sets of results are

in reasonable overall agreement with the available data. There is, therefore, no firm reason to discard *a priori* a plasma-like viewpoint for polyvalent simple metals, provided, of course, that the appropriate coupling strength is scaled down to values similar to those for monovalent metals.

Acknowledgments

This work was sponsored by the Ministero dell'Università e della Ricerca Scientifica e Tecnologica of Italy through the Consorzio Interuniversitario Nazionale di Fisica della Materia. We are very grateful to Professor S K Lai for providing us with effective pair potentials for polyvalent metals. OA and ZB wish to thank Professor Abdus Salam, the International Atomic Energy Agency and UNESCO for grants allowing their participation in the Condensed Matter Physics programmes at the International Centre for Theoretical Physics in Trieste.

References

- [1] Feynman R P 1972 *Statistical Mechanics* (New York: Benjamin) p 46
- [2] Ashcroft N W and Stroud D 1978 *Solid State Physics* vol 33, ed F Seitz, D Turnbull and H Ehrenreich (New York: Academic) p 1
- [3] Umar I H, Meyer A, Watabe M and Young W H 1974 *J. Phys. F: Met. Phys.* **4** 1691
- [4] Lai S K, Matsuura M and Wang S 1983 *J. Phys. F: Met. Phys.* **13** 2033
- [5] Carnahan F and Starling K E 1969 *J. Chem. Phys.* **51** 635
- [6] Ashcroft N W and Lekner J 1966 *Phys. Rev.* **165** 83
- [7] Minoo H, Deutsch C and Hansen J P 1977 *J. Physique* **38** L191
- [8] Ross M, DeWitt H E and Hubbard W B 1981 *Phys. Rev. A* **24** 1016
- [9] Young W H 1982 *J. Phys. F: Met. Phys.* **12** L19
- [10] Lai S K 1988 *Phys. Rev. A* **38** 5707
- [11] Baus M and Hansen J P 1980 *Phys. Rep.* **59** 1
- [12] DeWitt H E, Slattery W L and Stringfellow G S 1990 *Strongly Coupled Plasma Physics* ed S Ichimaru (Amsterdam: Elsevier) p 635
- [13] Mon K K, Gann R and Stroud D 1981 *Phys. Rev. A* **24** 2145
- [14] Singh H B and Holtz A 1983 *Phys. Rev. A* **28** 1108
- [15] Singh H B and Holtz A 1984 *Phys. Rev. A* **29** 1554
- [16] Hoshino K 1984 *J. Phys. Soc. Japan* **53** 4279
- [17] Lai S K 1985 *Phys. Rev. A* **31** 3886
- [18] Hoshino K and Young W H 1986 *Phys. Chem. Liquids* **15** 229
- [19] Joarder R N and Bari A 1986 *Physica B* **142** 161
- [20] Joarder R N and Das T 1988 *Phys. Scr.* **37** 762
- [21] Iwamatsu M 1989 *Physica B* **159** 269
- [22] Lai S K, Akinlade O and Tosi M P 1990 *Phys. Rev. A* **41** 5482
- [23] Akinlade O, Lai S K and Tosi M P 1990 *Physica B* **167** 61
- [24] Palmer R G and Weeks J D 1973 *J. Chem. Phys.* **58** 4171
- [25] Badirkhan Z, Pastore G and Tosi M P 1991 *Mol. Phys.* **74** 1089
- [26] Hansen J P and Weis J J 1977 *Mol. Phys.* **33** 1379
- [27] Rosenfeld Y and Ashcroft N W 1979 *Phys. Rev. A* **20** 1208
- [28] Verlet L and Weis J J 1972 *Phys. Rev. A* **5** 939
- [29] Henderson D and Grundke E W 1975 *J. Chem. Phys.* **63** 701
- [30] Li D H, Li X R and Wang S 1986 *J. Phys. F: Met. Phys.* **16** 309
- [31] Li D H, Moore R A and Wang S 1987 *J. Phys. F: Met. Phys.* **17** 2007
- [32] Singwi K S, Sjölander A, Tosi M P and Land R H 1970 *Phys. Rev. B* **1** 1044
- [33] Ichimaru S and Utsumi K 1981 *Phys. Rev. B* **24** 7385
- [34] Gillan M J 1979 *Mol. Phys.* **38** 1781

- [35] Abernethy G M and Gillan M J 1980 *Mol. Phys.* **39** 839
- [36] Hansen J P 1973 *Phys. Rev. A* **8** 3096
- [37] Penfold R, Nordholm S, Jönsson B and Woodward C E 1991 *J. Chem. Phys.* **95** 2048
- [38] van der Lugt W and Alblas B P 1985 *Handbook of Thermodynamic and Transport Properties of Alkali Metals* ed R W Ohse (Oxford: Blackwell)
- [39] Waseda W 1980 *The Structure of Non-Crystalline Materials* (New York: McGraw-Hill)